ELM Mitigation by Supersonic Molecular Beam Injection into the H-mode Pedestal in HL-2A Tokamak

W.W. Xiao[1,2], P.H. Diamond[2,3], X.L. Zou[4], J.Q. Dong[1,5], X.T. Ding[1], L.H. Yao[1], B.B. Feng[1], C.Y. Chen[1], W.L. Zhong[1], M. Xu[3], B.S. Yuan[1], T. Rhee[2], J.M. Kwon[2], Z.B. Shi[1], J. Rao[1], G.J. Lei[1], J.Y. Cao[1], J. Zhou[1], M. Huang[1], D.L. Yu[1], Y. Huang[1], K.J. Zhao[1], Z.Y. Cui[1], X.M. Song[1], Y.D. Gao[1], Y.P. Zhang[1], J. Cheng[1], X.Y. Han[1], Y. Zhou[1], Y.B. Dong[1], X.Q. Ji[1], Q.W. Yang[1], Yi Liu[1], L.W. Yan[1], X.R. Duan[1], Yong Liu[1] and HL-2A team

[1] *Southwestern Institute of Physics, P.O. Box 432, Chengdu, China*

[2] *WCI Center for Fusion Theory, National Fusion Research Institute, Daejeon, 305-333, S. Korea*

[3] *UCSD, San Diego, California 92093, USA*

[4] *CEA, IRFM, F-13108 Saint-Paul-lez-Durance, France*

[5] *Institute for Fusion Theory and Simulation, Zhejiang University, Hangzhou, China*

Emai: xiaoww@swip.ac.cn

Abstract:

Density profiles in pedestal region (H-mode) are measured in HL-2A and the characteristics of the density pedestal are described. Cold particle deposition by Supersonic Molecular Beam Injection (SMBI) within the pedestal is verified. ELM mitigation by SMBI into the H-mode pedestal is demonstrated and the relevant physics is elucidated. The sensitivity of the effect to SMBI pressure and duration are studied. Following SMBI, the ELM frequency increases and ELM amplitude decreases for a finite duration period. Increases in ELM frequency of $f_{ELM}^{SMBI} / f_{ELM}^{0}$ ~ 2-3.5 are achieved. This experiment argues that the ELM mitigation results from an increase in

higher frequency fluctuations and transport events in the pedestal, which are caused by SMBI. These inhibit the occurrence of large transport events which span the entire pedestal width. The observed change in the density pedestal profiles and edge particle flux spectrum with and without SMBI supports this interpretation. An analysis of the experiment and a model shows that ELMs can be mitigated by SMBI with shallow particle penetration into the pedestal.

PACS numbers: 52.55Fa, 52.25.Fi, 52.35.Ra, 52.40.Mj

1. Introduction

Since the H-mode was first discovered in the ASDEX tokamak [1], more than a quarter-century of related studies has followed [2]. H-mode is characterized by an edge pedestal or edge transport barrier (ETB) as it is manifested on the profiles of the plasma density and temperature. In ELMy H-mode, the plasma edge is a region of crucial importance due to its influence on plasma confinement and performance. ELMy H-mode exhibits fast, quasiperiodic short bursts called edge localized modes (ELMs), which eject particles and energy from plasma. The loss of energy leads to large quasiperiodic power impulses on the divertor target, which can cause significant erosion [3]. A central question for ITER [4] is whether external control tools can be developed to reduce the ELM size to acceptable values while maintaining good confinement. An effective control scheme should show an increase in the actual ELM frequency relative to the intrinsic ELM frequency f_{ELM}. Since the relation $f_{ELM} \times \Delta W_{ELM} \approx \text{const.}$, with ΔW_{ELM} the energy loss per ELM [5, 6], holds for intrinsic ELMs on many diverted tokamaks, increasing the frequency should decrease W_{ELM}^{0}, as we desire. Existing techniques for ELM control or mitigation include pellet pacing [7], nitrogen seeding injection [8,9], RMP [10] and other external perturbation fields [11]. Both such physics problems require tuning the macroscopic

relaxation oscillations of a self-organized criticality which can manifest spatiotemporal chaos and cyclic bursts. In particular, the aim of ELM control is to eliminate the largest transport events, which cause the largest impulsive heat loads on the divertor.

In this work we describe a novel experimental demonstration of ELM mitigation by SMBI, and elucidate the physics of this result. The organization of this article is as follows: the experiment parameters and the density pedestal structure are presented in the second part. The third section gives the confirmation of the cold particle source deposition. The fourth part presents the important experimental results of ELM mitigation by Supersonic Molecular Beam Injection (SMBI) and some analysis of the experiments is given and a simple model is discussed. In this section, the comparison of the experimental results and the model for the particle source deposition in ELM mitigation by SMBI are presented as well. The last part is the summary.

2. Experimental description of basic parameters and key diagnostics

The HL-2A is a middle size (R=1.65m, a= 0.40m) tokamak [12]. Some advanced diagnostic systems such as microwave reflectometry (MWR) [13], ECE and Thomson scattering have been installed in the HL-2A tokamak in recent years. A variety of fuelling techniques (SMBI, Extruded Pellet Injector with 40 pellets, Gas Puffing) have been developed and improved in this machine.

The H-mode experiments (Type-III and Type-I like ELMs [14, 15]) were conducted in HL-2A since 2009. The general discharge parameters are plasma current I_P= 140kA - 200 kA, toroidal magnetic field strength B_t= 1.2 - 1.5 T and line average density 1.8-2.3$\times 10^{19}$m^{-3}, respectively. Besides Ohmic plasma heating, auxiliary heating by electronic cyclotron resonance heating

(ECRH, the available heating power ~ 0.9-1.6 MW) and neutral beam injection (NBI, the available heating power ~ 0.3-0.8 MW) was used [16, 17]. The total output power of heating system is about 2-2.5 MW. The pedestal structure was measured by the reciprocating Langmuir probe and the microwave reflectometry [18]. SMBI system was used for the first time in the HL-2A tokamak [19]. This SMBI system has particular virtues: 1) a well defined pulse period, 2) localized deposition of the injected particles and 3) well controlled particle penetration. Some significant experiments, such as the density perturbation for particle transport study and particle transport barrier [20, 21], have been conducted using this tool. ELM mitigation, resulting from particle penetration into the pedestal region by SMBI, is realized for the first time.

O-mode broadband microwave reflectometry system (MWR) has been installed at the mid-plane of the torus at LFS. It has been successfully operated in HL-2A since 2004 [13]. In this system, there are four main parts: 1) the fast scanning microwave source, 2) the wide band modulator, 3) the reflection signal detector and 4) the inphase/quadrature modulation (I/Q) system. The time resolution of the reflectometry system is less than 1 *ms* and the spatial resolution is about several *mm*. A full density profile of the edge plasma can be measured using MWR and a fast reciprocating Langmuir probe system (RLP) [22] with 8 *cm* scan from the scrape-off layer to the plasma boundary in HL-2A. The density pedestal can be measured by RLP and MWR. In this campaign, generally, the height of the density pedestal is about $1.2\times10^{19}m^{-3}$, the width is about 3cm and the pedestal density gradient scale length is about 2cm, respectively. A detailed description of density pedestal in H-mode discharge is presented for shot 14052 as shown in figure 1. In (a), the blue curve is the line averaged density and the black and red dash lines are the specially chosen time for density profiles. The gray bars are the ECRH and NBI

heating power and heating duration time (ECRH heating duration 424-824 ms and NBI heating duration 516-916 ms). The available heating power of ECRH is about 920 kW and the available heating power of NBI is about 320 kW in this shot 14052. (b) is the D_α ELM monitor as type-III ELMs and (c) is a zoom in from 630 to 680 ms for the D_α ELM monitor. (d) is the density profile in Ohmic regime and H-mode phase. A clear density pedestal structure is measured by MWR and RLP [18]: the width (W_{ped}) is about 2.8 cm, the height (n_{ped}) is about 1.25×10^{19} m^{-3}, which is 60% of line-averaged density (2×10^{19} m^{-3}) and the pedestal density gradient scale length (L_n) is about 2cm. Here the squares are the results by RLP and the triangles and circles are measured by MWR at 350ms (only Ohmic regime) and 650ms (H-mode regime with ECRH and NBI heating), respectively, as shown in (a). The density profile by MWR in H-mode phase shows that it is measured without ELM burst, as shown in (c). The separatrix, which is calculated by current filaments (CF) code with the filament current model [23, 24], is at 37.2cm as shown by the green dash line in figure 1 (d).

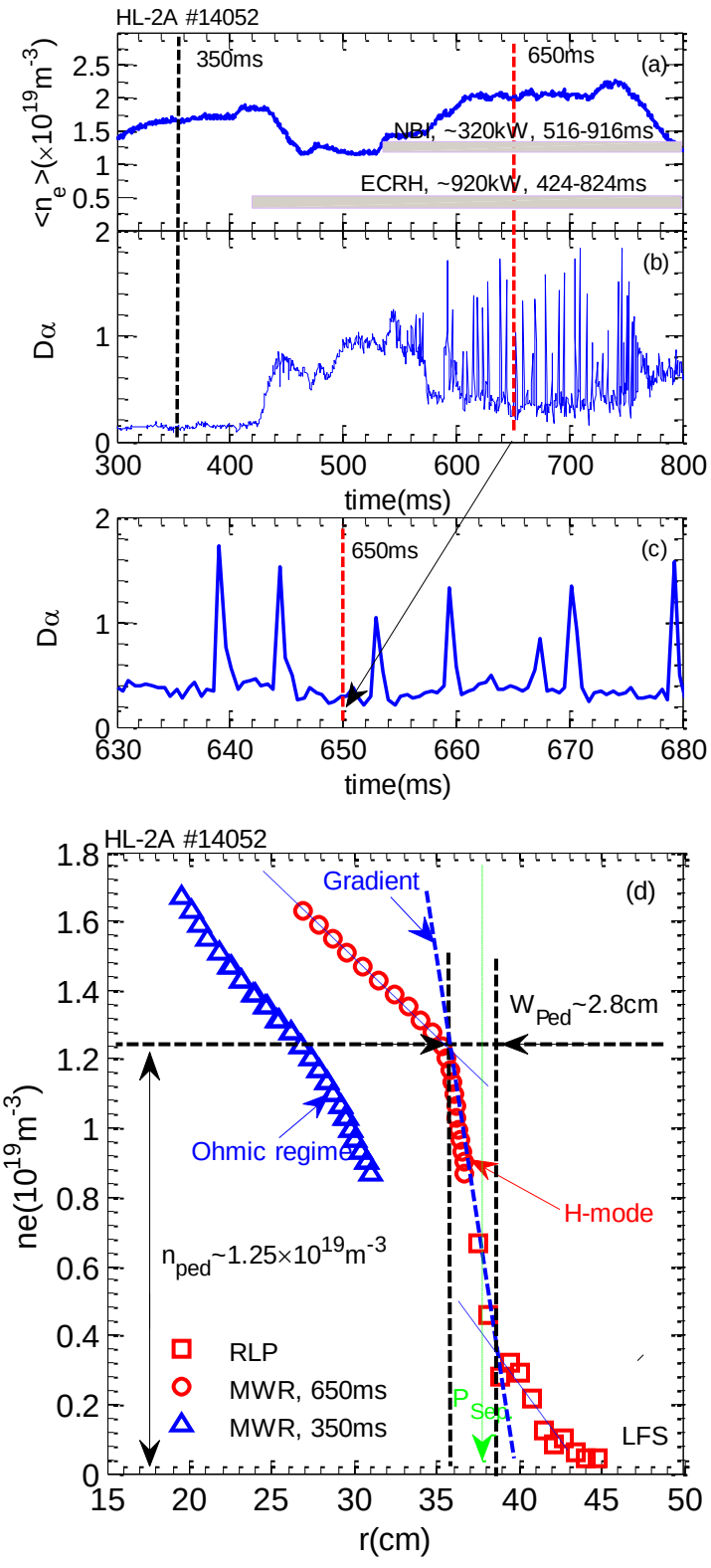

Figure 1. A detailed description of density pedestal in H-mode discharge for shot 14052. (a) is the line averaged density and heating power. Two specially chosen times are shown with the black and red dash lines. (b) is the D_α ELM monitor. (c) is a zoom in from 630 to 680 ms for the

D_α ELM monitor. (d) is the density pedestal structure for this shot: the width (W_{ped}) is about 2.8 cm, the height (n_{ped}) is about 1.25 $\times$ 10^{19} m^{-3} and the pedestal density gradient scale length (L_n) is about 2cm.

3. Particle source confirmation in H-mode phase

It is very important to know the particle source position in order to interpret the ELM mitigation experiment by SMBI. Some ELM trigger experiments have reported that the pellet needs to be sufficiently large (and fast) to penetrate close to the pedestal top [25]. A local particle source can be determined by three means: 1) the minimum of the phase of the first harmonic of Fourier transform of the modulated density measure using microwave reflectometry, 2) the maximum of the D_a intensity, 3) the maximum of the derivative of the density in time at the beginning of the density modulation, when the density evolution is dominated by the particle source. The method to confirm particle source has been evidenced in [20]. If one of the three means above can be obtained, the cold particle source position for one SMBI pulse can be confirmed using the rate of density increase with time $\partial_t n_e$. Figure 2 shows the particle position by SMBI in Ohmic discharge for shot 3875. In this case, the particle source deposited by SMBI is centered about r~28cm and the particle penetration depth is deeper than that by the general gas feed [26, 27], such as gas puffing.

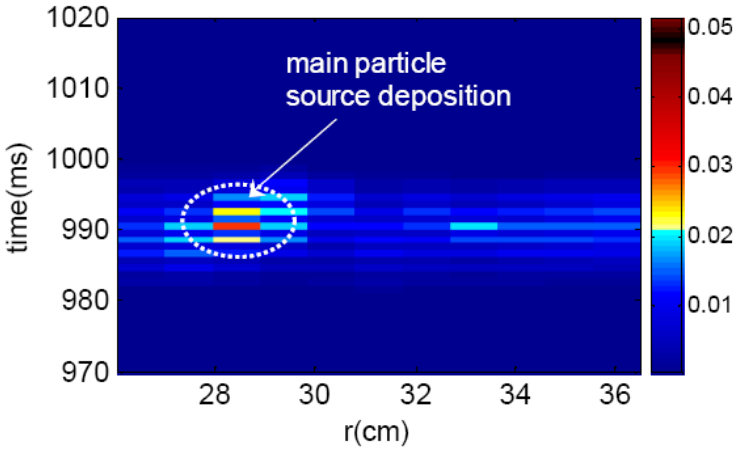

Figure 2. The particle source position in Ohmic discharge. The amplitude is the rate of increase of plasma density at different radii for shot 3875. Main particle source deposite at *r*~28cm.

In same way, deposition of neutral gas (Deuterium) into the pedestal via SMBI is achieved in H-mode discharges. Figure 3 shows the density profile by MWR for shot 14045 at 665ms and a SMBI pulse was injected at this time. The gas presure of the SMBI system is about 1.3MPa, SMBI duration is 3ms and the line average density is about 2×10^{19}m^{-3}. The pedestal height is about 1.17×10^{19}m^{-3} and the pedestal top postion is at 35.7 cm as shown the arrow in figure 3. The particle source position is confirmed as shown in figure 4 due to $\partial_t n_e$. In figure 4 (a) and (b), there is a sharp variation around *r* ~37.2cm for H-mode shot 14045. The separatrix position is ~ 37.4 cm, while the density pedestal top postion has been measured in figure 3, as show by the dash line in figure 4 (a). It indicates that the injected cold particles are indeed deposited just inside of the separatrix, as shown in the white ellipse in figure 4 (a) and 3-*D* by the profile of $\partial_t n_e$ in space-time as shown the arrow direction in figure 4 (b). It is very clear that this particle source position is shallower than for the Ohmic case is compared to figure 2.

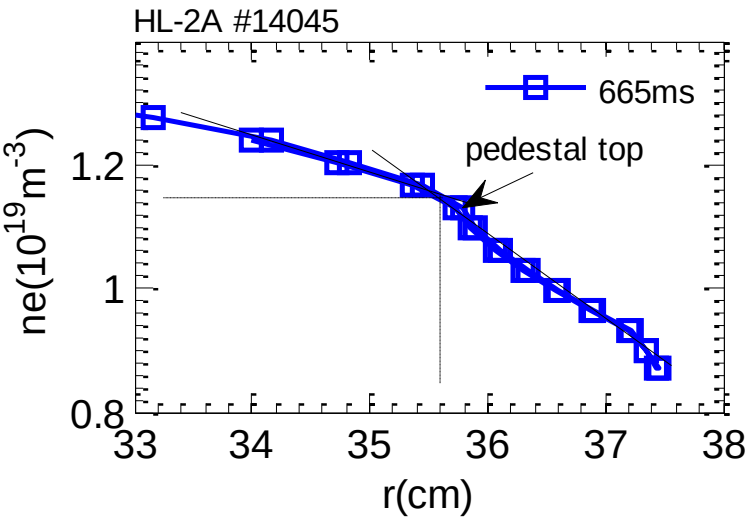

Figure 3. Denstiy pedestal top position is 35.7cm for shot 14045 and a SMBI pulse was injected at 665ms.

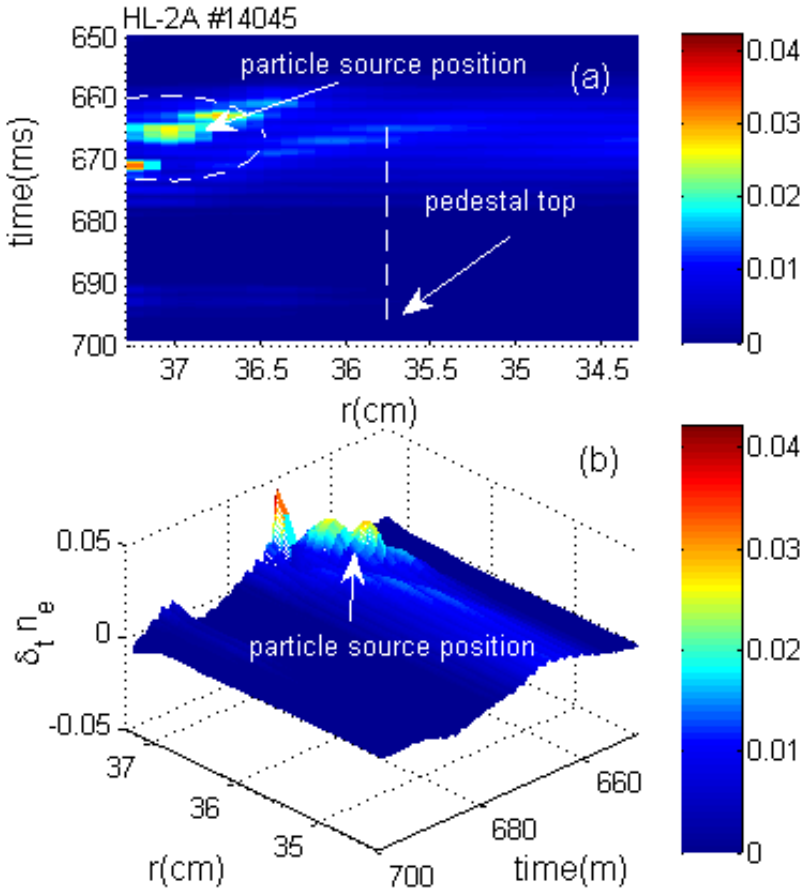

Figure 4. The cold particle source position by one injected SMBI pulse was confirmed using the rate of density increase with time for H-mode shot 14045. The separatrix is at 37.4 cm and the density pedestal top is about 35.7 cm. (a) is the contour map of the rate of density increase and (b) is the 3-*D* profile of the $\partial_t n_e$ in space-time. The particle source position is noted by arrows.

4. ELM mitigation experiments by SMBI

4.1 Experimental results on ELM mitigation by SMBI

An ELM mitigation experiment is feasible with shallow cold source deposition in the pedestal region as described above. Figure 5 shows the principal experimental results of ELM mitigation by SMBI. The ELM frequencies f_{ELM} with and without SMBI are shown in this figure by square and circle, respectively. The frequency f_{ELM}^{SMBI} with SMBI is larger than f_{ELM}^{0} without SMBI. The increase in frequency of $f_{ELM}^{SMBI} / f_{ELM}^{0}$ is about 2-3.5. Auxiliary heating power is about 0.9-1.4MW and $< n_e >$ is about 1.8-2.3$\times 10^{19}$m^{-3} for these discharges.

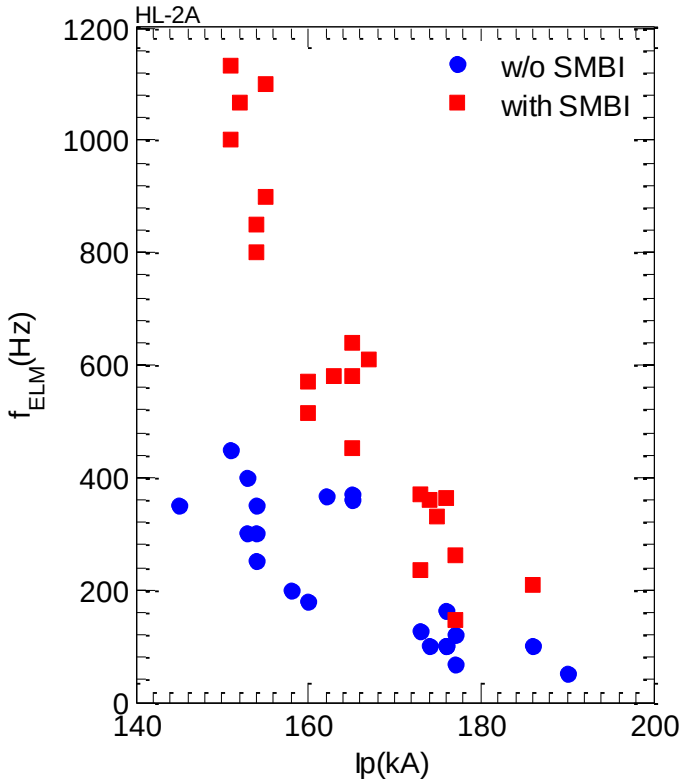

Figure 5. The H-mode discharge in principal experimental results of ELM mitigation by SMBI. ELM frequency f_{ELM} with and without SMBI are presented by squares and circles, respectively. The increase factor in frequency of $f_{ELM}^{SMBI} / f_{ELM}^{0}$ is about 2-3.5.

A typical ELM mitigation by SMBI is investigated for shot 15886 as shown in figure 6. From top to bottom: (a) is the electromagnetic valve control signal of SMBI system, τ_{pulse} is the duration of the nozzle work time as shown in figure 6 (a). (b) is the D_a signal and the τ_I is about 20 ms. Here, τ_I means the SMBI influence time, i.e. the duration of the increase in f_{ELM} and associated ELM amplitude decrease, thus, τ_I is set by the time to re-fill the pedestal density after it is perturbed by SMBI and its meaning is shown as the double arrow between both dashed lines. A clear difference of the ELM frequency and ELM amplitude with and without SMBI can be observed. The ELM frequency increases while the ELM amplitude decreases. (c) is the interval between ELMs and (d) is the ELM amplitude evolution. Based on the red and black lines in (d) and (d), the $f_{ELM}^{SMBI} / f_{ELM}^{0}$ is about 3.2 and ELM amplitude decreases by about 1/3 after one SMBI pulse. (e) is the total energy confinement time. From this curve, we can get the information that the total confinement time is almost unchanged by SMBI. It means that ELM mitigation by SMBI can be achieved and that plasma confinement is not destroyed in the process. This key point is also our principal result. The bottom box (f) is the line averaged density by HCN in this shot. During the SMBI influence time τ_I, there is a slight density increase with SMBI fueling. In this box, comparison of the density change by the ELM burst with and without SMBI among three zones I, II and III, it was found that the macroscopic change of the line averaged density is clear: density curve is smoothed in zone II due to the small ELMs, on the contrary, the density curve has clear change in zones I and III. The line averaged density change explicitly indicates that the effect of ELM mitigation by SMBI.

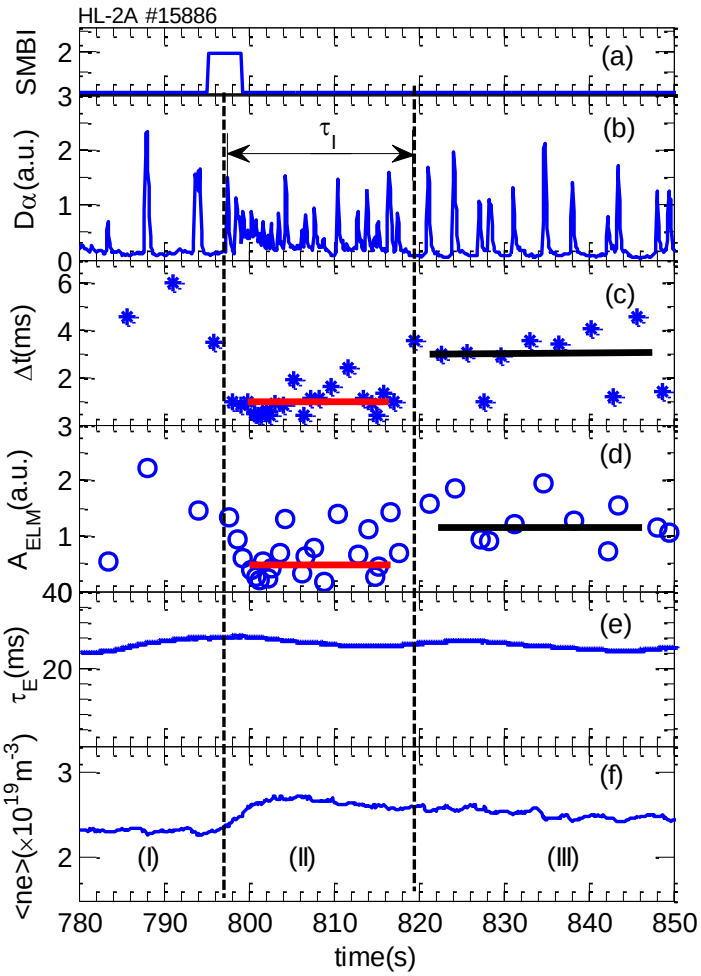

Figure 6. The experimental results of ELM mitigation using SMBI. (a) is the electromagnetic valve control signal of SMBI system. (b) is the D_a ELM monitor, here, τ_I means the SMBI influence time. Its meaning is shown as the double arrow. (c) is the interval between ELMs and (d) is the ELM amplitude evolution. (e) is the total energy confinement time and (f) is the line averaged density by HCN.

4.2 Experimental parameters chosen for the SMBI system for ELM mitigation

We must note that there is no ELM mitigation effect if the SMBI duration is too short ($\leq$2ms) or the gas pressure is too low ($\leq$1.1 MPa), as shown in figure 7. In this case, there is no obvious density profile change in the pedestal region (r_{sep}~36.8cm) for shot 16233 in HL-2A. This means the cold particle source deposition is outside of the pedestal, so that the cold particles can't

penetrate the pedestal region. Figure 7 shows D_a signal and SMBI electron magnetic control signal of the SMBI system. It is clear that there is no change for the D_a signal, period and amplitude, even SMBI injection at 450 ms and 505ms.

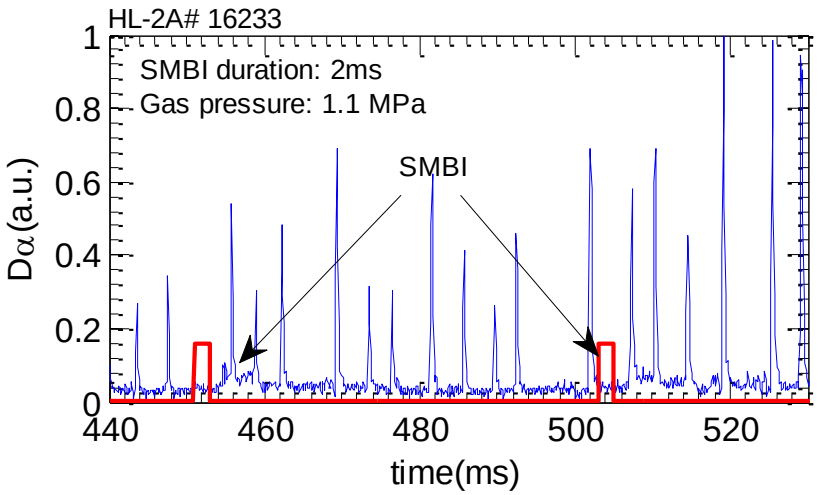

Figure 7. The D_a signal and SMBI electromagnetic valve control signal of the SMBI system for shot 16233. There is no change for the D_a signal, period and amplitude, even with SMBI injection.

Comparative experiments proved that no SMBI pulse with a too low gas pressure nor a too short duration can not achieve ELM mitigation. Optimized ELM mitigation experiments have been successfully conducted as shown by figure 8, which presents the relation between individual SMBI pulse duration τ_{pulse} and the SMBI persistence influence time τ_I. For the gas pressure of 1.1 MPa in figure 7 (a), there is no effect of ELM mitigation for 2ms SMBI duration as shown the star mark, while ELM mitigation effects appear for 4 ms and 6 ms SMBI duration. However, for gas pressure of 2.0 MPa in figure 8 (b), the ELM mitigation effect with 4 ms SMBI duration is more striking than that for 2 ms SMBI duration. For the ELM mitigation by SMBI, the optimized parameters of the SMBI are the gas pressure of 2 MPa and the pulse duration τ_{pulse} of 4 ms for the HL-2A tokamak.

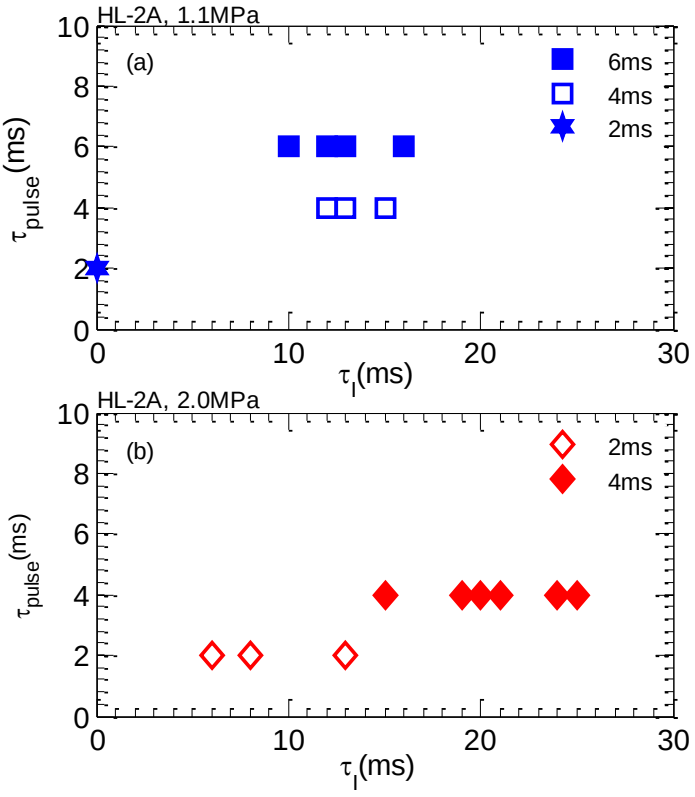

Figure 8. The relation between SMBI duration τ_{pulse} and τ_I in 1.1 MPa (a) and in 2.0 MPa (b).

4.3 *Experimental analysis for ELM mitigation by SMBI*

The density profile is measured by a broadband O-mode Microwave reflectometry in HL-2A [13]. Density profile analysis shows a distinct difference in pedestal density gradient steepness when comparing the profiles with and without SMBI cases. Figure 9 shows the (a) is the electromagnetic valve control signal of SMBI system, (b) the D_a ELMs monitor and (c) the density profiles at different times 701 ms, 722 ms and 737 ms. These correspond to the times indicated in (b) by the arrows. In figure 9 (c), the density profiles clearly change due to SMBI. It shows that the density gradient softens (i.e. becomes less steep) immediately following SMBI (722ms, L_n=3.3cm). Before SMBI injection, the density gradient (701ms, L_n=2.2cm) is steeper

than with SMBI (722ms, L_n=3.3cm). Similar result for the steeper density gradient is measured at 737ms. After a large ELM, the density gradient is observed to steepen significantly (737ms, L_n=2.2cm). These observations mean that the pedestal particle confinement is degraded by SMBI injection. An approach to a possible explanation has been presented in [28], and the key point of this result is that SMBI deposition in the pedestal inhibits the formation of the largest, most extended transport events which span the full width of the pedestal. This comes at the expense of an increase in the population of smaller fluctuations and avalanches. Thus SMBI mitigates ELMs but increases the turbulent particle flux.

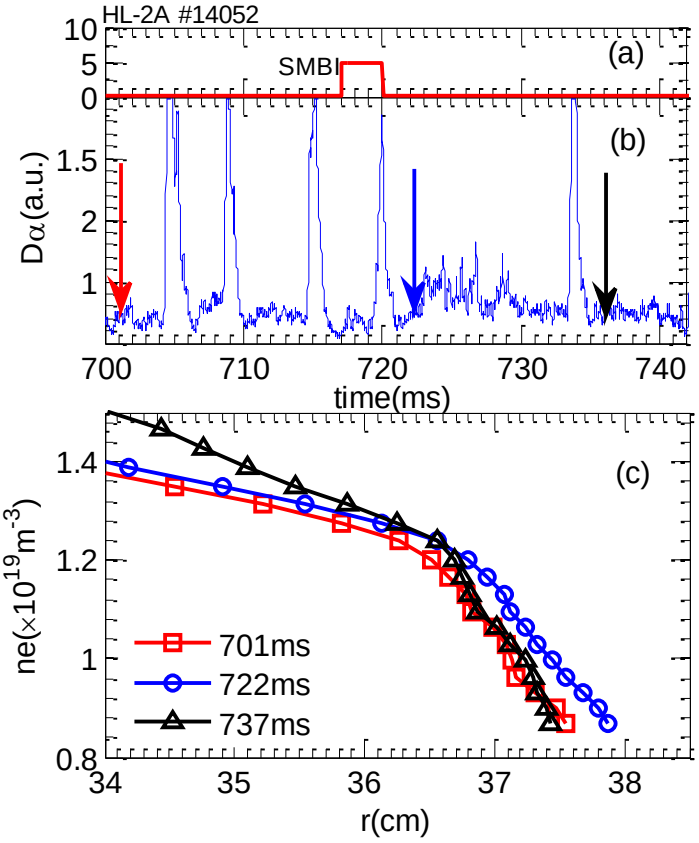

Figure 9. ELM mitigation results and density profiles. (a) is the electromagnetic valve control signal of SMBI system, (b) is the ELMs signal and (c) is the density profiles at with SMBI (722ms) and without SMBI (701ms and 737 ms.

A change in the spectrum of edge particle flux is indeed observed during ELM mitigation experiments, as shown in figure 10. (a) is the electron magnetic control signal of SMBI system and there is a SMBI pulse injection at 698 ms. (b) is the D_α ELM monitor and the SMBI influence time τ_I is about 25 ms, as shown the double arrows. (c) is the particle flux and the particle flux ($<\tilde{\upsilon}_r * \tilde{n}>_f / n_0$) spectrum was measured using Langmuir probe in HL-2A [19]. The $<\tilde{\upsilon}_r * \tilde{n}>_f / n_0$ comparison of Langmuir probe measurements of the edge particle flux with and without SMBI is shown. Here, $\tilde{\upsilon}_r$ is the radial velocity perturbation, $\tilde{n}$ is the density perturbation and n_0 is the equilibrium density. The red curve is after SMBI injection and blue curve is before SMBI injection for shot 16246 (The SMBI parameters in this shot: τ_{pulse}=4ms and gas pressure is 2.0MPa). In figure 10 (b), the time windows of the data by Langmuir probe has been marked with the blue (A) and red (B) bars and corresponding durations are 650-670 ms without SMBI case and 715-735 ms with SMBI, respectively. It is clear that with SMBI, the low frequency (f<8kHz) content of the edge particle flux spectrum decreases (the red curve B) in (c), while there is some indication that the higher frequency (f>8kHz) content increases. This is consistent with the idea that SMBI inhibits the formation of large (low frequency) avalanches or transport events, while triggering more small (high frequency) avalanches [28]. This is also consistent with the observed reduction in pedestal density gradient with SMBI in figure 9 (c) the blue density profile at 722 ms.

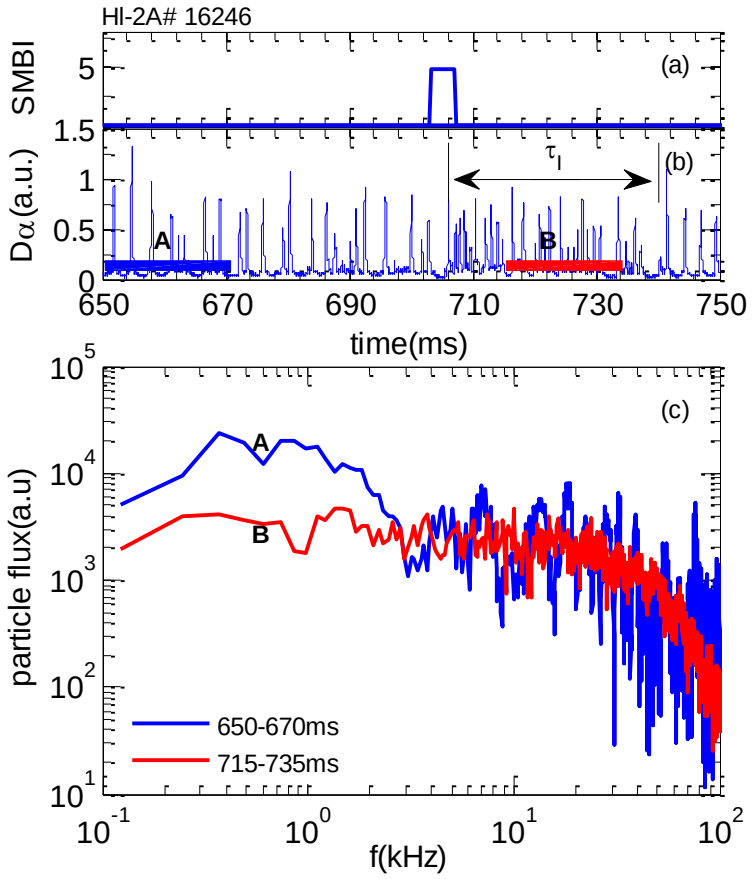

Figure 10. Comparative results of the fluctuation driven particle flux measured 1cm (1-2 radial correlation lengths) outside for the separatrix for shot 16246. Red curve B and blue curve A are the cases of with and without SMBI, respectively.

We calculate the integral areas of the ELM amplitude [29] using trapezoidalintegration for both with and without SMBI cases as shown in figure 11. The blue one is without SMBI case (ELM frequency 450 Hz) and the integral of the ELMy amplitude is 6044.5 (a.u.). The red one is with SMBI case (ELM frequency 800 Hz) and the integral of ELMs is 6689.5 (a.u.). The average error of the areas of the ELM amplitude for both cases is less than 6% even the ELM burst is a complex and nonlinear process, including MHD, turbulence transport and energy particle, etc. The comparison of the areas indicates that intensities of the D_a emission with and without SMBI are close, thus the relation $f_{ELM} \times \Delta W_{ELM} \approx \text{const.}$ [6, 30] holds in this experiment through the

estimate areas of ELM amplitude as well. It is also a key point for ITER to reduce the ELM size to an acceptable levele and keep good confinement [31].

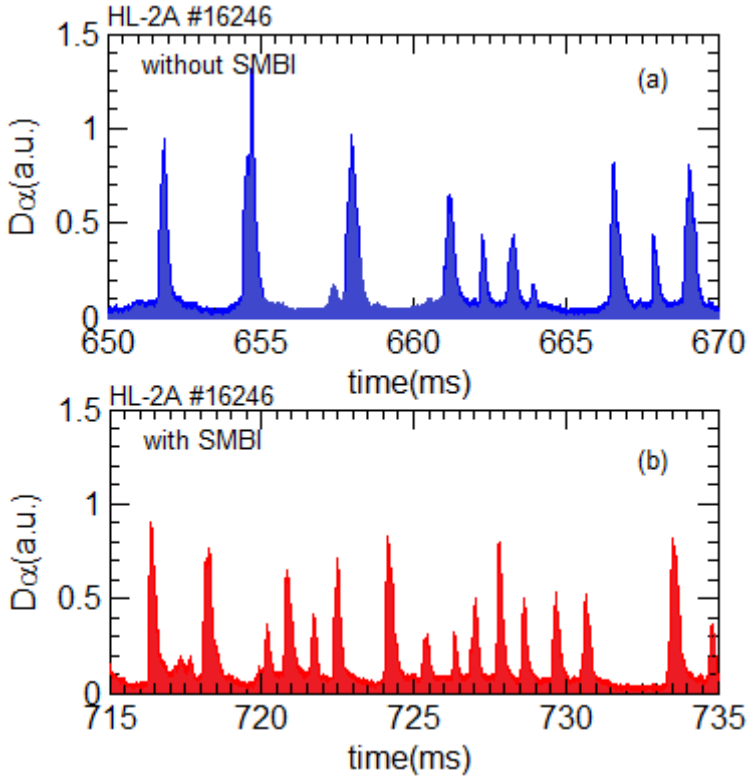

Figure 11. Calculation of the area contained in per ELM for the case with (red, bottom) and without (blue, top) SMBI. In the case without SMBI the ELM frequency is 450 Hz, and the integral area of the ELM amplitude is 6044.5 (a.u.). The ELM frequency is 450 Hz and the integral of the ELM amplitude is 6044.5 (a.u.). In the case with SMBI, the ELM frequency is about 800 Hz, and the integral area of ELM amplitude is 6689.5 (a.u.). The average error of the areas of the ELM amplitude is less than 6% in both cases.

4.4 Simple model analysis for the ELM mitigation experiment

We have extensively studied the effect of SMBI-like pulsed grain deposition in the pedestal region of a sand pile model which exhibits ELM-like ejection events. The basic model is described in ref [28, 32] and consists of a sand pile with ejecting boundary on one side, a bi-

stable toppling rule, noise-driven scattering to emulate collision diffusion, and an ultimate upper hard threshold for relaxation of the gradient, to emulate the MHD stability boundary related trigger for ELM events. In particular, we emphasize that the model of ref [27] incorporates an automaton rule (i.e. turbulence mixing prescription linking local scattering and redistribution to local gradient), which includes both i) a bi-stable soft rule, which captures the critical element of pressure gradient feedback acting to reduce transport and ii) a hard upper local gradient limit, which emulates the effect of a macroscopic instability. The model also includes constant diffusion, to emulate neoclassical transport. Though exceedingly simple, this model captures the basic dynamical trends of an ELMy H-mode pedestal. ELMs occur when the entire edge pedestal region is populated up to the hard threshold limit, and occur as ejection events driven by avalanches which span the full pedestal cross-section. We have performed a series of numerical experiments to test the effect of additional pulsed grain injection within the pedestal, in order to mimic and study SMBI effects on ELMs. Figure 12 shows the results. Large ejection events (ELMs) are clearly manifested without additional injection. Using a finite series of additional injections at the edge of pedestal, the ELM amplitude drops precipitously while the ELM frequency increases (figure 12 (b)). A similar trend is observed when the additional injection is applied deeper into the pedestal base, though the amount of reduction is not as large (figure 12 (c)). Interestingly, the apparent synchrony between injection and ejection observed for edge injection is not for so apparent for deeper injection.

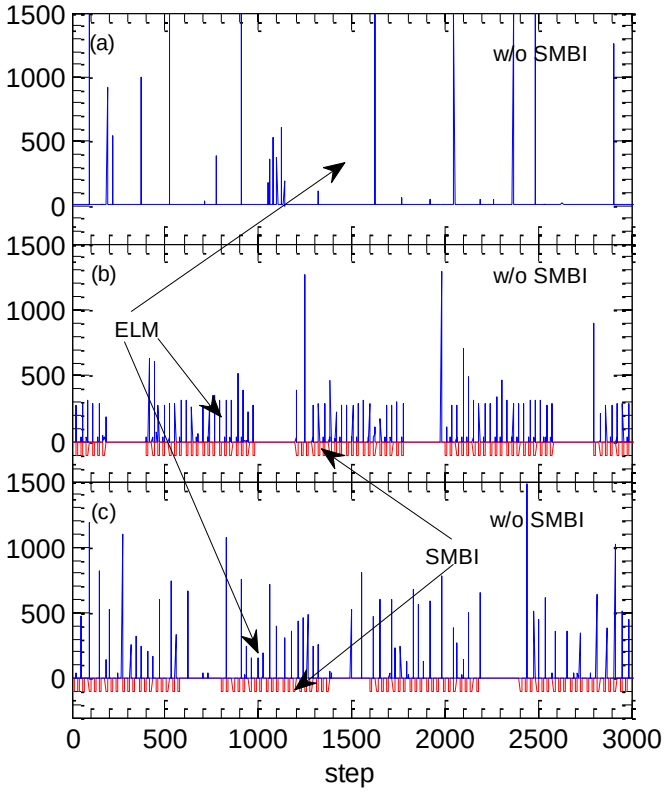

Figure 12. Ejection flux time evolution with additional grain injection: (a) without injection, (b) edge injection and (c) pedestal base injection.

Figure 13 shows at the results of an ejection event census, i.e. the number of ejection avalanches of a certain size, as measured by the duration of the avalanche (in the number of successive edge toppling). Results without additional injection are compared to those for various pulse durations. The simulations clearly show that additional injection (as for SMBI) reduces the population of large avalanches while increasing the population of smaller avalanches. Note that shorter pulse duration (τ_{pulse} =20, 40 for figure 13) is more effective than longer duration. Also, comparison of figure 13 (a) with (b) shows that deposition deeper inside the pedestal mitigates, but does not eliminate large ELMs. *These results suggest that near edge deposition with modest pulse length is optimal for ELM mitigation.* The basic physical mechanism for ELM mitigation by SMBI is that electron temperature drops with SMBI so perhaps resistive MHD might be at

work, at the same time SMBI changes the relative distribution of transport events, generating much smaller avalanches which inhibits the formation of larger ELMs [32].

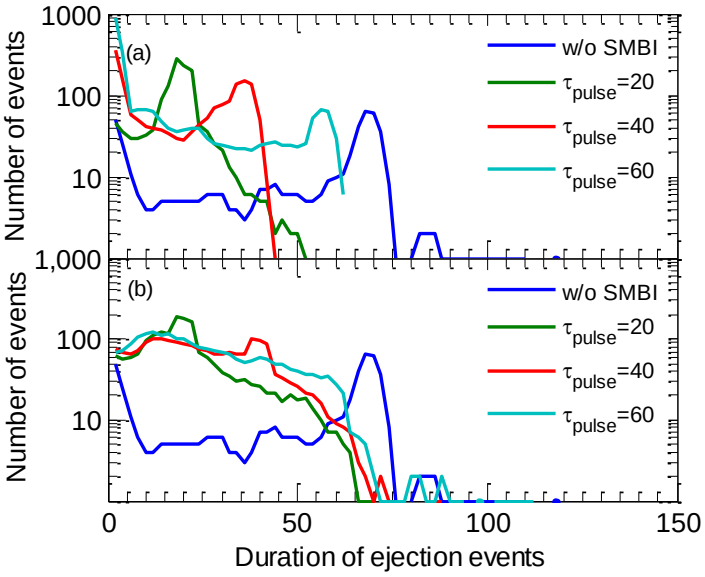

Figure 13. Distribution of ejection events. x-axis is duration of ejection (i.e. event size), and y-axis is the number of events. (a) is edge injection and (b) is deeper injection.

This conclusion is supported by figure 14, which shows that the contours of relative increase in ELM frequency f_{ELM}/f_{ELM}^{0} vs deposition point $0<x<1$ in pedestal region and deposition size y - $\delta n/n$. Clearly, the best results are achieved for $x\sim 0.8$, inside the pedestal, but close to the outer edge. It indicates that *deep penetration of the pedestal is not necessary.*

The trends indicated by this simplified model study are all qualitatively consistent with the experimentally observed trends, and *suggests that shallow SMBI deposition into the pedestal mitigates ELMs by reducing the population of large avalanche transport events, while increasing the number of smaller events.* We believe this mechanism to be fundamentally different from that of pellet pacing (pp). In pp, deeper injection of a closely timed series of small pellets coherently

synchronizes the ELM cycle to the pellet injection cycle, thus increasing the ELM frequency while decreasing the amplitude. In pp the basic physics remains the same, but the pellets 'pick up the pace'. In SMBI mitigation, large spontaneous ejection events and ELMs are reduced by stimulating a broad spectrum of smaller scale mixing and transport events. There is no need for synchrony and the dynamics are incoherent. The number of injected particle is small. Plasma density does not increase in time.

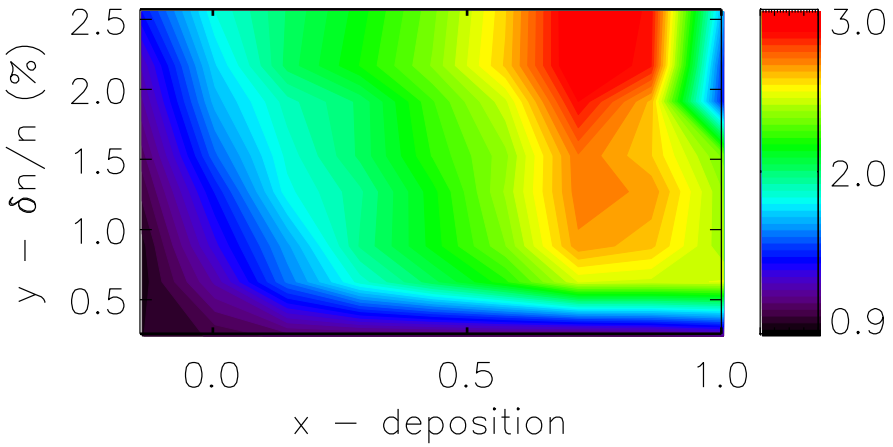

Figure 14. Contour plot of the frequency of ejection events normalized by the frequency without additional grain injection (i.e. *f/f(0)*). x-axis is the injection location in pedestal width (0<x<1) and y-axis is the number of additional grains divided by the pedestal line averaged density.

4.5 Comparison of experiment and model

General pedestal structure has been obtained in HL-2A. The height is about $1.2\times10^{19}m^{-3}$ and the width is about 3cm. SMBI pulse can penetrate the separatrix and deposit the material on the foot of the density pedestal region, as shown in figure 4. For shot 14045, the main particle source position is about 37.3cm and density pedestal top position is about 35.7cm. We take the pedestal width is about 2.8cm, so pedestal outside boundary is 38.5cm. The change value of pedestal

density due to one SMBI pulse injection into the pedestal is about 10% in HL-2A and the fundamental position of the particle source based on experiment can be obtained in normalized pedestal domain under ρ_{ped}, as shown in figure 15. So, the main particle source position is about ρ_{ped}~0.6 in pedestal width and the pedestal density change due to SMBI pulse is shown in this figure as the vertical axis. Here, δn_e is the local variation of density due to SMBI injection and n_{e-ped} is the local pedestal density. Comparison of the simple model, the optional particle source from this model is about ρ_{ped}~0.8 , as shown in figure 14. It indicates that the particle source is about outside of the half pedestal domain ρ_{ped}. There is a small deviation between experimental results and the model analysis, but both results support the important conclusion: it is not necessary to deposit the SMBI pulse source at the pedestal top. Deposition just inside the foot of the pedestal is sufficient for the ELM mitigation by SMBI. The similar achievement of the ELM mitigation or control by pellet is given in [33]. It indicates that the ITER requirement for LFS fuelling injection to reach the top of the pedestal may be overly conservative. The particle deposition may need to penetrate just inside the separatrix in ITER in order to mitigate or control the ELMs.

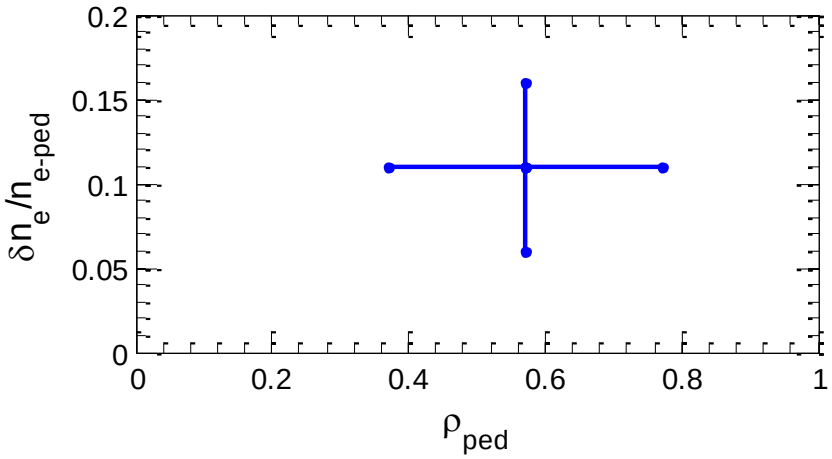

Figure 15. Particle source position is outside of the half pedestal domain ρ_{ped} for ELM mitigation

by SMBI.

5. Summary

Clear density pedestal structure was confirmed in HL-2A. ELM mitigation was achieved by SMBI pulse injection into pedestal region. ELM mitigation was achieved by SMBI pulse injection into pedestal region. The experimental results show that the frequency and the amplitude of ELMs can be actively controlled using SMBI and the relation $f_{ELM} \times \Delta W_{ELM} \approx \text{const.}$ is evidenced. One optimized SMBI influence time is about 20-25ms. A degradation density gradient scale length L_n is measured during the SMBI pulse injection. Based on the change in edge particle flux spectrum by Langmuir probe, the comparison of particle source position on the experiment and the simple theoretical model, it indicates that the particle source is about outside of the half pedestal domain ρ_{ped}. Thus, we conclude that deep penetration of the pedestal is not necessary for ELM mitigation by SMBI. The SMBI deposition just inside the separatrix appears sufficient to trigger small transport events and so mitigate large ELMs. This suggests that the prospects for ELM mitigation using fuelling in ITER are positive.

The authors would like to thank X.Q. Xu, M. Kikuchi, C. Xiao, S.W. Yoon and S.H. Hahn for fruitful discussions. This work is supported by Chinese National Fusion Project for ITER under Grant No 2009GB104007, and the Nos. 10990213, 10975049 and 11175056, also Korea WCI project 2009-0001. It is also partially supported within the framework of the cooperation between the French Commissariat à l'Energie Atomique et aux Energies Alternatives (CEA) and the China National Nuclear Corporation (CNNC).

References

[1] F. Wagner et al., 1982 Phys. Rev. Lett. 49, 1408

[2] F. Wagner, 2007 Plasma Phys. Control. Fusion 49, B1

[3] ASDEX team, 1989 Nucl. Fusion 29, 1959

[4] ITER Physics Basis Editors ,et al. 1999 Nucl. Fusion 39 2137

[5] A. Herrmann, 2002 Plasma Phys. Control. Fusion 44, 883

[6] A Herrmann, 2002 Plasma Phys. Control. Fusion 44, 883

[7] P.T. Lang et al., 2003 Nucl. Fusion 43, 1110

[8] J Rapp et al., 2002 Plasma Phys. Control. Fusion 44, 639

[9] Y Corre et al., 2008 Plasma Phys. Control. Fusion 50 115012 (20pp)

[10] Y. Liang et al., 2007 Phys. Rev. Lett. 98, 265004

[11] M.J. Schaffer et al., 2008 Nucl. Fusion 48, 024004

[12] X.R. Duan et al., 2009 Nucl. Fusion 49, 104012

[13] W.W. Xiao et al., 2006 Plasma Sci. Technol. 8, 133

[14] X.R. Duan et al., 2010 Nucl. Fusion 50, 095011

[15] Y. Huang et al., 2010 37th EPS Conference on Plasma Phys. Dublin, June 21-25, P-2.136, Dynamics of Edge Localized Modes in the HL-2A tokamak, http://ocs.ciemat.es/EPS2010PAP/pdf/P2.136.pdf

[16] J. Rao et al., 2009 Nuclear Fusion and Plasma Physics 4 324 (in Chinese).

[17] G.J. Lei et al., 2009 36th EPS Plasma Physics Conference June 29 - July 3 Sofia, Bulgaria, The Progress of NBI heating experiment on HL-2A, http://epsppd.epfl.ch/Sofia/pdf/P5_148.pdf

[18] L.W. Yan, eta l., 2011 Nucl. Fusion 51 094016 (8pp)

[19] L.H. Yao, et al., 2001 Nucl. Fusion 41, 817

[20] W.W. Xiao et al., 2010 Rev. Sci. Instrum. 81, 013506

[21] W.W. Xiao et al., 2010 Phys. Rev. Lett. 104, 215001

[22] L.W. Yan et al., 2005 Rev. Sci. Instrum. 76, 093506

[23] A. Allgeyer, ASDEX, 1974 Proc. 8th Symposium on Fusion Technology, 317

[24] B.S. Yuan, et al., 2005 Nuclear Fusion and Plasma Physics, 25, 1 (in Chinese)

[25] P.T. Lang, et al., 2011 Nucl. Fusion 51 033010 (16pp).

[26] L.H. Yao, et al., 2007 Nucl. Fusion, 47 1399

[27] L.H. Yao, 2006 New Developments in Nuclear Fusion Research, edited by Y. Nakamura (Southwestern Institute of Physics, Chengdu, China), chap. 3, pp. 61–87

[28] I. Gruzinov, P. H. Diamond and M. N. Rosenbluth, 2002 Phys. Rev. Lett. 89, 25; Phys. Plasma, 2002 10, 569

[29] T.E. Evans et al., 2006 Nature physics, 2 419

[30] G. D. Porter, T. A. Casper, and J. M. Moller, 2001 Phys. Plasma, 8 5140

[31] E J Doyle et al. Progress in the ITER Physics Basis Chapter 2: Plasma confinement and transport 2007 Nucl. Fusion 47 S18

[32] T. Rhee, J.M. Kwon, P.H. Diamond and W.W. Xiao, 2012, Phys. Plasma, 19 022505

[33] L.R. Baylor, et al., 2010 37th European Physical Society Conference on Plasma Physics, 20-21st June, Dublin, Ireland, p2. 117, ELM pacing by pellet injection on DIII-D and extrapolation to ITER, http://ocs.ciemat.es/EPS2010PAP/pdf/P2.117.pdf